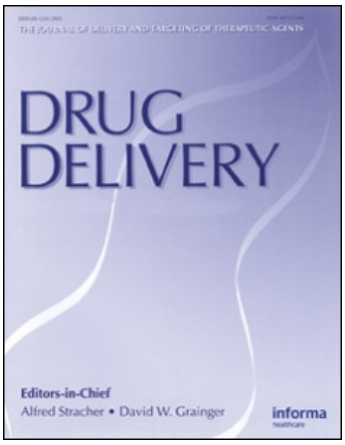

Drug Delivery
Publication details, including instructions for authors and subscription information:
http://www.informaworld.com/smpp/title~content=t713769758

Polyelectrolyte Biomaterial Interactions Provide Nanoparticulate Carrier for Oral Insulin Delivery

Catarina Pinto Reis [a]; António J. Ribeiro [a]; Francisco Veiga [a]; Ronald J. Neufeld [b]; Christiane Damgé [c]
[a] Laboratory of Pharmaceutical Technology, Faculty of Pharmacy, University of Coimbra, Portugal [b] Department of Chemical Engineering, Queen's University, Kingston, Ontario, Canada [c] Institute of Physiology, Faculty of Medicine, University Louis Pasteur, Strasbourg, France

Online Publication Date: 01 February 2008

To cite this Article Reis, Catarina Pinto, Ribeiro, António J., Veiga, Francisco, Neufeld, Ronald J. and Damgé, Christiane(2008)'Polyelectrolyte Biomaterial Interactions Provide Nanoparticulate Carrier for Oral Insulin Delivery',Drug Delivery,15:2,127 — 139

To link to this Article: DOI: 10.1080/10717540801905165

URL: http://dx.doi.org/10.1080/10717540801905165

Drug Delivery, 15:127–139, 2008

ISSN: 1071-7544 print / 1521-0464 online
DOI: 10.1080/10717540801905165

informa
healthcare

Polyelectrolyte Biomaterial Interactions Provide Nanoparticulate Carrier for Oral Insulin Delivery

Catarina Pinto Reis, António J. Ribeiro, and Francisco Veiga
Laboratory of Pharmaceutical Technology, Faculty of Pharmacy, University of Coimbra, Portugal

Ronald J. Neufeld
Department of Chemical Engineering, Queen's University, Kingston, Ontario, Canada

Christiane Damgé
Institute of Physiology, Faculty of Medicine, University Louis Pasteur, Strasbourg, France

Nanospheres are being developed for the oral delivery of peptide-based drugs such as insulin. Mucoadhesive, biodegradable, biocompatible, and acid-protective biomaterials are described using a combination of natural polyelectrolytes, with particles formulated through nanoemulsion dispersion followed by triggered *in situ* gel complexation. Biomaterials meeting these criteria include alginate, dextran, chitosan, and albumin in which alginate/dextran forms the core matrix complexed with chitosan and albumin coat. Smaller size and higher albumin-based acid-protective formulation was orally administered to diabetic rats and glucose reduction and physiological response analyzed. Insulin encapsulation efficiency was 90, 82, and 66% for uncoated, chitosan-coated, and albumin-chitosan-coated alginate nanospheres, respectively. The choice of coating polymer seems to influence insulin release profile and to be crucial to prevent peptic digestion. Physiological response following oral delivery showed that insulin albumin-chitosan-coated alginate nanospheres reduced glycemia ∼72% of basal values. Albumin serves as an important enteric coating providing acid- and protease protection enabling uptake of active drug following oral dosage.

Keywords Nanospheres, Insulin, Polyelectrolyte complexes, Oral Delivery

Diabetes mellitus type 1 is a generalized disorder of glucose metabolism that is generally attributed to an absence of insulin secretion. The unique treatment remains periodic insulin injection, a poor approximation of normal physiological insulin secretion. While oral administration of insulin is a potentially attractive option, success at delivery via this route has thus far been elusive. Insulin, like other peptide- or protein-based drugs, is degraded in the acidic environment of the stomach and by proteolytic enzymes, especially in the small intestine. In addition, epithelial surfaces and chemical characteristics of the gastrointestinal tract present an effective barrier to the absorption of insulin (Reis et al. 2002a). Numerous strategies have been devised to enhance insulin absorption. Nanoparticles as a drug delivery system have been found to be useful in protecting and/or prolonging insulin effect (Damgé, Maincent, and Ubrich 2007; Jerry et al. 2001; Mesiha, Sidhom, and Fasipe 2005). In the nanotechnology field, polymeric biomaterials have been received increasing attention, especially gastric and proteolytic protective polymers.

Alginate is a natural biodegradable polymer that gels in the presence of divalent cations such as calcium. Alginate gel is relatively permeable and thus has a low retention capacity of encapsulated molecules (Gursoy and Cevik 2000). The low retention capacity is due probably to an open pore structure that depends on the extent of swelling and contraction of the alginate gel. There have been numerous efforts to control the erosion of alginate and prolong drug release such as coating with polycationic polymers or blending alginate with other polymers (Lee et al. 2003). Dextran sulfate is a biodegradable and biocompatible polyanion, with a branched carbohydrate backbone and negatively charged sulfate groups (Chen, Mohanraj, and Parkin 2003). It has been widely used in pharmaceutical formulations as an effective matrix material for controling release of drugs (Janes et al. 2001) or as a stabilizing agent (Tiyaboonchai et al. 2003).

Chitosan is a nontoxic and bioabsorbable natural polysaccharide, with structural characteristics similar to glycosaminoglycans (Hari, Chandy, and Sharma 1996). It has been studied

Received 10 May 2007; accepted 15 July 2007.
The authors are grateful for financial support from the *Fundação para a Ciência e Tecnologia*, Portugal (SFRH/BD/13673/2003), *Hospitais da Universidade de Coimbra*, and from the *Natural Sciences and Engineering Research Council of Canada*. The authors thank Dr. Alcino Leitão for his kind help in FT-IR studies.
Address correspondence to Catarina Pinto Reis, Laboratory of Pharmaceutical Technology, Faculty of Pharmacy, University of Coimbra, Rua do Norte, 3000-295 Coimbra, Portugal. E-mail: catarinareis@ci.uc.pt

for the release of several drugs or as a gel coating material as its polymeric cationic characteristics promote interaction with negatively charged molecules or polymers (Boonsongrit, Mitrevej, and Mueller 2006). Moreover, chitosan adheres to the mucosal surface and transiently opens the tight junction between epithelial cells. Finally, most polypeptide drugs such as insulin are short-lived species *in vivo*. In contrast, BSA is a stable protein *in vivo* (Schechter et al. 2005). BSA has been described as a model encapsulated drug. In this study, bovine serum albumin (BSA) was used as coating biomaterial with the intent of prolonging particle residence in the gastrointestinal tract and to provide protection of the entrapped insulin from intestinal proteases.

The aim of our study was to prepare and characterize polyelectrolyte nanospheres that can encapsulate, protect and biologically deliver insulin to intestinal mucosa. Polyelectrolyte nanospheres were produced through nanoemulsion/dispersion of alginate-drug solution, followed by triggered *in situ* gelation of alginate through instantaneous release of Ca^{2+} from insoluble complex. The nanoparticulate core was then coated with chitosan and/or albumin. Uncoated (ALG), chitosan-coated alginate (ALG-CHIT) and albumin-chitosan-coated alginate (ALG-CHIT-BSA) nanospheres were prepared and characterized in terms of size, chemical and thermal complex interactions, encapsulation efficiency, protein integrity after pepsin digestion, and physiological response following oral delivery in diabetic rats.

MATERIALS AND METHODS

Low viscosity sodium alginate (viscosity of 2% solution at 25°C, 250 cps), chitosan (50 kDa, 75–85% deacetylated), BSA, and streptozotocin were purchased from Sigma-Aldrich Chimie (L'Isle d'Abeau Chesnes, France). Dextran sulfate (5 kDa) and emulsifier, Span 80, were purchased from Fluka Biochemika (Buchs, Switzerland). Setacarb calcium carbonate was obtained from Omya (Orgon, France). Paraffin oil was supplied by Vaz Pereira (Lisbon, Portugal). Insulin was kindly donated by *Hospitais da Universidade de Coimbra* (Actrapid Insulin® from Novo Nordisk, Bagsvaerd, Denmark). All other chemicals were of reagent grade or equivalent.

Preparation of Nanospheres

Nanosphere preparation involved formulation of alginate particles through nanoemulsion dispersion followed by triggered instantaneous particle gelation (Reis et al. 2002b). A solution with sodium alginate (2%, w/v) and dextran sulfate as adjuvant (0.75%, w/v) was prepared by stirring (100 rpm) overnight. Insulin was then added and dissolved (100 IU/mL, 10 mL). An aqueous suspension of ultrafine calcium carbonate (5%, w/v) was added to previous alginate solution and the dispersion was emulsified within paraffin oil aided by Span 80 emulsifier (1.5% v/v) at high speed (1600 rpm). After 15 min, gelation was induced by addition of 20 mL paraffin oil containing glacial acetic acid to solubilize calcium dispersed in the alginate nanodroplets. After 60 min, an acetate buffer solution (pH 4.5, *United States Pharmacopeia [USP XXVIII]*) with dehydrating solvents (100 mL) was added to the oil-nanoparticle suspension and nanospheres were recovered by centrifugation (12,500 × *g* during 10 min) as previously described (Reis et al. 2006c).

Formulation coating variables were investigated for optimization of nanospheres properties by individually changing the preparation conditions in the described standard protocol with all other parameters held constant. All types of polymers and their concentration except BSA were based on previous works (Reis et al. 2007; Silva et al. 2006). First-coating strategy included chitosan coating (volume 100 mL at pH 4.5, 0.03% [w/v]) with high calcium level ($CaCl_2$ at 1.5%, w/v) applied under magnetic stirring during 30 min. Then, supernatant with unreacted polymer was removed by vacuum. The other strategy involved an additional coating of BSA (0.5–2% BSA [w/v] in 100 mL at pH 5.1) applied under magnetic stirring during 30 min. Nanospheres were frozen in an ethanol bath at −50°C and lyophilized (Lyphlock 6, Labconco, Kansas City, MO, USA) at 0°C for 48 h and stored at 4°C without cryoprotectant. These particles were referred to as dehydrated nanospheres. Insulin-free nanospheres also were prepared.

Characterization of Nanospheres

Size distribution was determined by laser diffraction spectrometry using a Coulter LS130 granulometer (Beckman Coulter, Fullerton, CA, USA). Mean diameters of nanosphere suspensions in acetate buffer pH 4.5 were determined in triplicate. Polydispersity was expressed as SPAN $= [D_{90\%} - D_{10\%}]/D_{50\%}$, where $D_{90\%}$, $D_{10\%}$, and $D_{50\%}$ are number size diameters at 90, 10, and 50% of the cumulative number, respectively. A high value of SPAN indicates a wide distribution in size and a high polydispersity. The shape of the particles also was characterized using scanning electron microscopy (SEM) (JSM-840, JEOL Instruments, Tokyo, Japan). Hydrated particles were dried by spray-drying and then deposited on metal grids using double-faced adhesive and coated with gold before observation.

Differential Scanning Calorimetry (DSC)

DSC was used to determine a shift of the alginate endothermic peak or the appearance of exothermic peaks and consequently detect interactions between ALG-CHIT and ALG-CHIT-BSA. Thermograms were obtained using a Shimadzu DSC-50 system (Shimadzu, Kyoto, Japan).

Sodium alginate, chitosan, and BSA were obtained by lyophilization of aqueous solution of alginate 2% (w/v), aqueous solution of chitosan 0.03% (w/v) rich in calcium ($CaCl_2$ at 1.5%, w/v), and aqueous solution of BSA 0.5 to 2% (w/v), respectively. Physical mixture was prepared by mixing 1:1 of lyophilized sodium alginate 2% (w/v) with chitosan 0.03% (w/v) rich in calcium ($CaCl_2$at 1.5%, w/v) and then by mixing 1:1 lyophilized ALG-CHIT with BSA 0.5 to 2% (w/v). Chitosan–alginate complexes were obtained by adding 5 mL of chitosan solution 0.03% (w/v) and rich in calcium ($CaCl_2$ at 1.5%, w/v) to 5 mL of

alginate solution 2% (w/v) at pH 4.5 under agitation for 10 min followed by lyophilization. BSA-chitosan–alginate complexes were obtained by adding 5 mL of BSA solution 0.5 to 2% (w/v) at pH 5.1 to 5 mL of chitosan solution 0.03% (w/v) and rich in calcium ($CaCl_2$ at 1.5%, w/v) with 5 mL of alginate solution 2% (w/v) at pH 4.5 under agitation for 10 min followed by lyophilization.

Coated-insulin nanospheres using different BSA concentrations were tested. Dehydrated samples (~2 mg) were crimped in a standard aluminium pan and heated from 20 to 350°C at a heating rate of 10°C/min under constant purging of nitrogen at 20 mL/min. The characteristic peaks of the melting endotherm and degradating exotherm were recorded. At least duplicates were carried out for each batch of sample and the results averaged.

Fourier Transform Infrared Spectrometry (FT-IR)

Infrared spectra of samples previously analyzed by DSC were recorded with a JASCO FT/IR-420 spectrophotometer (Miracle, PIKE® Technologies) using the attenuated total reflection method. Samples were scanned from 600 to 4000 cm^{-1} at a resolution of 4 cm^{-1}.

Encapsulation Efficiency

The encapsulation efficiency was measured by incubating 15 mg of dehydrated nanospheres in 10 mL of sodium citrate (55 mM)/phosphate buffer at pH 7.4 (*USP XXVIII*) for 1 hr (100 rpm). The pH of 7.4 was applied to produce higher protonation of insulin and alginate under simulated physiological conditions, and thus achieve low interaction between both chemical species. After particle dissolution, the mixture was centrifuged and protein content in supernatant analyzed by HPLC (Shimadzu, Columbia, MD, USA, LC-2010; where mobile phase was water (A): acetonitrile (B) with 0.04% trifluoroacetic acid with linear gradient B 30% to 40% over 5 min, flow rate 1.2 mL/min at 25°C) using reversed-phase column (X-Terra C-18 column, 5 μm, 4.6 mm × 250 mm from Waters, USA) with a precolumn (Purospher STAR, RP-18 precolumn, 5 μm, 4 mm × 4 mm from Merck, Germany). Encapsulation efficiency was determined by insulin released as percentage of initial amount used in formulation.

In Vitro Release of Insulin

Drug release studies were focused on the release behavior at gastric and intestinal pH conditions. Lyophilized insulin-loaded nanospheres (10 mg) were incubated in 10 mL hydrochloric acid buffer at pH 1.2 (*USP XXVIII*), under continuous magnetic stirring (100 rpm, 2 hr) at 37°C. Samples at appropriate intervals were withdrawn and assayed for protein. Fresh dissolution medium was added to maintain a constant volume. To simulate the progress of nanospheres moving from the stomach into the upper small intestine, the buffer was changed after 2 hr to higher pH. Nanospheres were centrifuged (12,500 × g, 10 min) then resuspended into 10 mL phosphate buffer at pH 6.8 (*USP XXVIII*), under continuous magnetic stirring (100 rpm) during 6 hr. Supernatant samples at appropriate intervals were withdrawn and assayed for protein, then fresh dissolution medium was added to maintain a constant volume. Experiments were performed in triplicate and cumulative insulin release expressed as percentage of initial insulin loading.

Insulin Molecular Integrity

Insulin (μg insulin per mL nanospheres) molecular integrity was evaluated by HPLC after nanospheres matrix dissolution with sodium citrate (55 mM)/phosphate buffer at pH 7.4 (*USP XXVIII*). Insulin was quantified initially and after 2 hr incubation in simulated gastric fluid containing pepsin at pH 1.2 (*USP XXVIII*) in a shaking water bath at 37°C and 100 rpm. Nanospheres were recovered by centrifugation and transferred to citrate solution in phosphate buffer 7.4 (*USP XXVIII*) with stirring for 1 hr, then aliquots collected, centrifuged, and analyzed. Phosphate buffer at pH 7.4 was applied to stop enzyme activity and to promote insulin release. Insulin encapsulated without pepsin incubation and nonencapsulated insulin served as reference and assays were conducted in triplicate. Enzyme resistance was detected by absence or presence of insulin peak on HPLC chromatogram.

In Vivo Bioassay of Optimized Nanospheres

The animal model chosen was the diabetic induced rat because it has several advantages over larger animals: easier manipulation, ability to simultaneously work with large number of animals, economical reasons, and mainly similarity to human diabetes histopathology (Lerco et al. 2003). Male *Wistar* rats (270 ± 24 g) were housed in a 12–12 hr light-dark cycle, constant temperature environment of 22°C, relative humidity 55%, and allowed free access to water and food during acclimatization. Animals received standard laboratory chow diet (UAR, Villemoisson-sur-Orge, France) and tap water, available *ad libitum*. All experiments were carried out in accordance with the European Community Council Directive of November 24, 1986 (86/609/EEC). Diabetes was induced with intravenous injection of 65 mg/kg streptozotocin in citrate buffer at pH 4.5 as previously described (Damgé et al. 1988). Then 10 days after the treatment, rats with frequent urination, loss of weight and fasting blood glucose levels higher than 300 mg/dL were included in experiments. Blood glucose levels were determined by glucose oxidase/peroxidase method using a glucometer (Accuchek Go, Roche, Strasbourg, France).

Animals were fasted 12 hr with free access to water and randomized in three groups: formulation (treatment with insulin-loaded nanospheres) and two controls (treatment with water and control insulin-free nanospheres). Water was selected as dispersion medium and for that reason it was tested as control. Only optimized nanospheres were administrated orally through a tube that was attached to a hypodermic syringe and approximately 2 mL of the aqueous dispersion medium was administered. Oral

TABLE 1
Size (nm) of tested formulations showing the effect of coating material and BSA concentration on $D_{10\%}$, $D_{50\%}$, $D_{90\%}$, and SPAN

Formulation	Parameter	D10%	D50%	D90%	SPAN
Dehydrated ALG nanospheres	ALG	358	564	1067	1.26
Dehydrated ALG-CHIT nanospheres	0.03% chitosan	741	1280	2652	1.49
Dehydrated ALG-CHIT-BSA nanospheres	0.5% BSA	110[a]	144[a]	392[a]	1.96
	1% BSA	110[a]	144[a]	298[a]	1.31
	1.5% BSA	110[a]	158[a]	298[a]	1.19
	2% BSA	110[a]	158[a]	298[a]	1.19
Hydrated ALG-CHIT-BSAnanospheres	1% BSA	392	677	1402	1.49

[a]High agglomeration.

dosage was 50 IU/kg of animal body weight. Optimized formulation was tested in dehydrated state and in the freshly prepared hydrated state. Blood samples were taken from the tip of the tail vein and blood-glucose curve was plotted.

Statistical Analysis

Data are presented as means ± standard error of mean (SEM). Statistical evaluation was performed with a one-way ANOVA followed by a Dunnett multiple comparison test. A $p < 0.05$ was taken as the criterion of significance.

RESULTS

Characterization of Nanospheres

Nanospheres were prepared by nanoemulsion dispersion/*in situ* triggered gelation resulting in an unimodal size distribution. Diameter values expressed in number distribution of nanospheres prepared using different formulation variables are presented in Table 1, as well as the SPAN factor, a measure of polydispersivity.

Approximately 50% of ALG and ALG-CHIT nanospheres showed a diameter of less than 564 and 1280 nm, respectively. SPAN factor values were 1.26 and 1.49 for ALG and ALG-CHIT nanospheres. ALG-CHIT-BSA nanospheres showed substantially lower particle sizes compared with ALG-CHIT and ALG nanospheres. An increasing concentration of BSA did not change the diameter. In contrast, the SPAN factor decreased with increasing concentration of BSA. ALG-CHIT nanospheres were regular and mainly spherical in shape as shown in Figure 1a) but coating with BSA resulted in particle shrinkage (Figure 1b) which is in agreement with size analysis.

DSC Analysis

DSC was used to characterize the polyelectrolyte complex interactions involving alginate, chitosan and BSA. Figure 2 shows broad and early endothermic peaks of BSA around 70°C and 220°C whereas exothermics peaks were localized at 320 and 370°C. When BSA was mixed with ALG-CHIT complexes, its spectra changed significantly as shown in Figure 3a and b): a broad endothermic peak between 60–70 and a new peak at 150°C that can be attributed to a strong interaction between polyelectrolytes with intensity increasing with increase of BSA. The exothermic peak of the ALG-CHIT complex was around

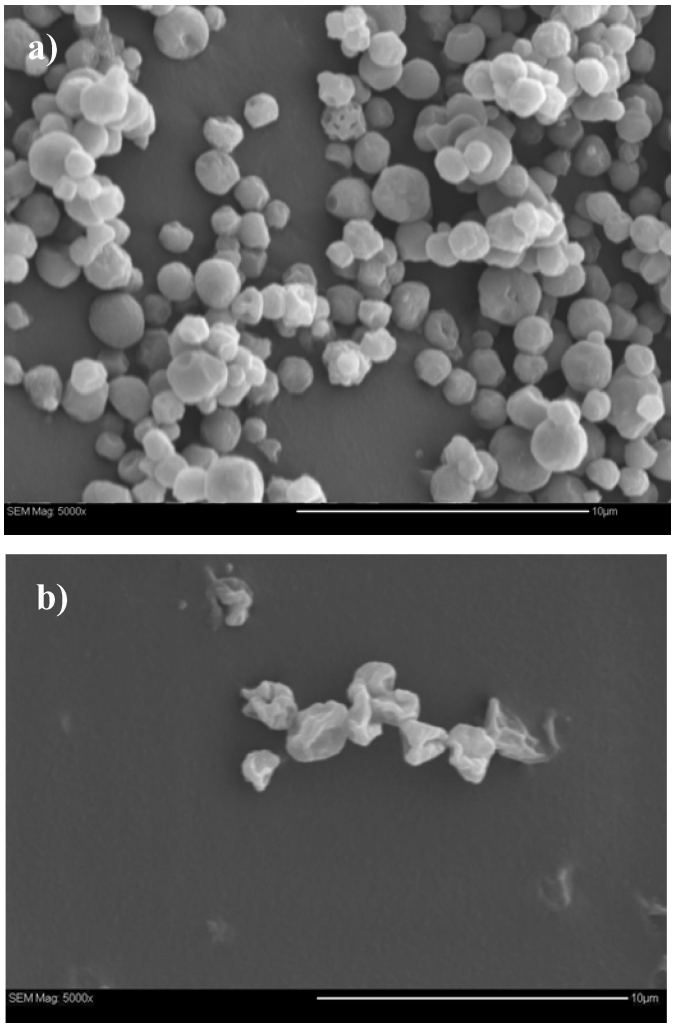

FIG. 1. SEM microphotographs of ALG-CHIT with 0.03% of chitosan (a) and ALG-CHIT-BSA nanospheres with 1% of BSA (b) (magnification 5000 ×, bars = 10 μm).

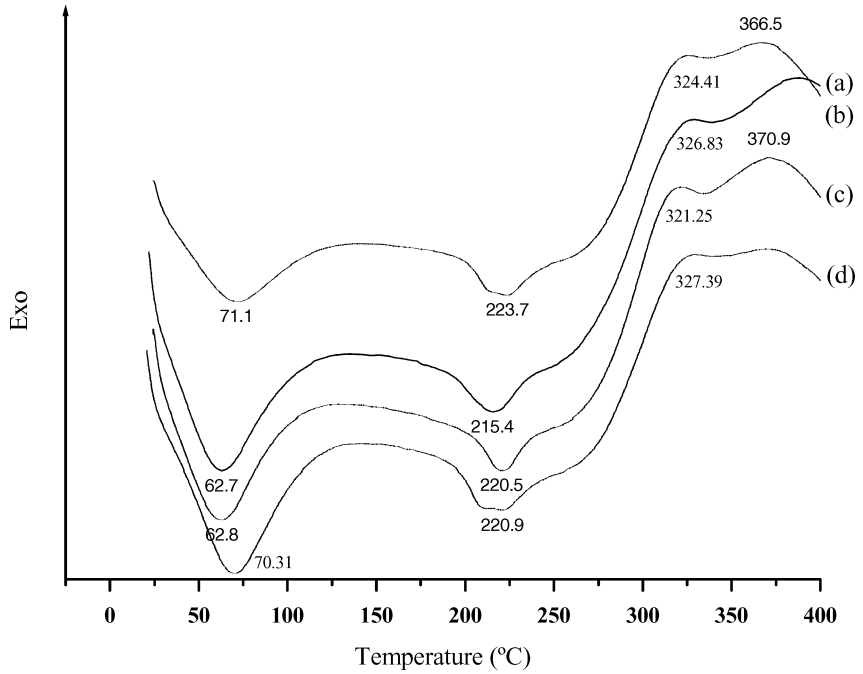

FIG. 2. Thermograms of dehydrated (a) 0.5%, (b) 1%, (c) 1.5%, and (d) 2% BSA.

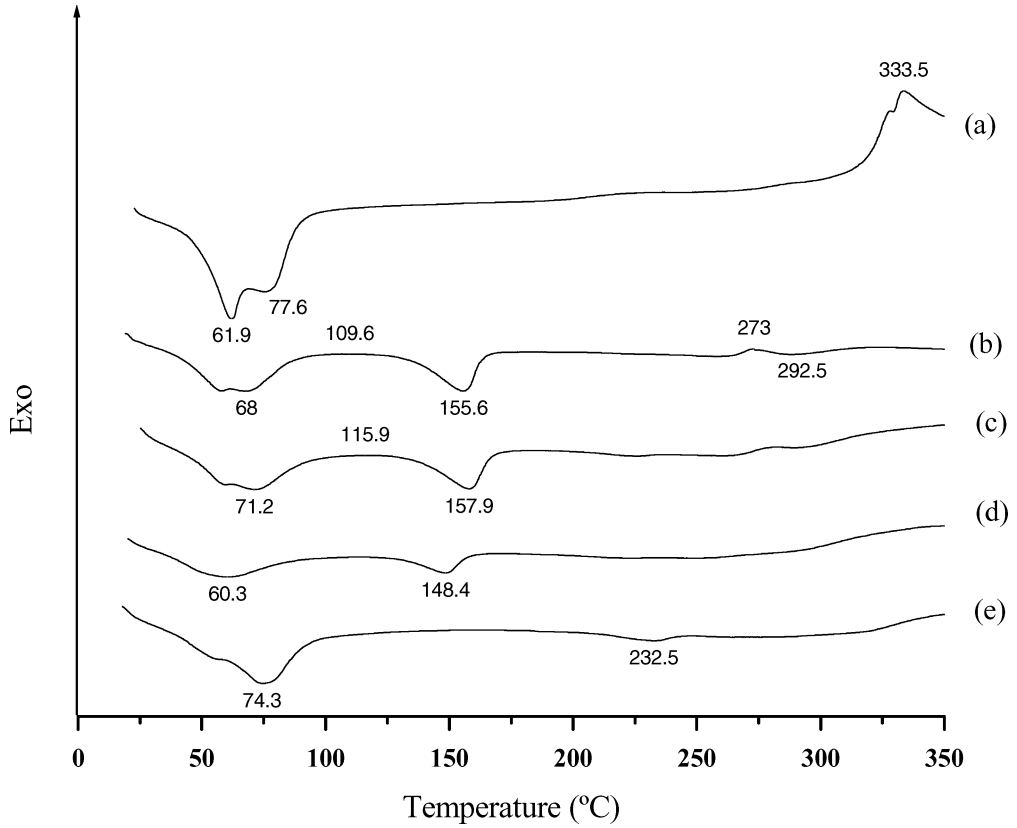

FIG. 3. Thermograms of dehydrated (a) ALG-CHIT complexes with 0.03% of chitosan and 2% of alginate; (b) ALG-CHIT-BSA complexes with 0.5% BSA; (c) ALG-CHIT-BSA complexes with 1% BSA; (d) ALG-CHIT-BSA complexes with 1.5% BSA; (e) ALG-CHIT-BSA complexes with 2% BSA.

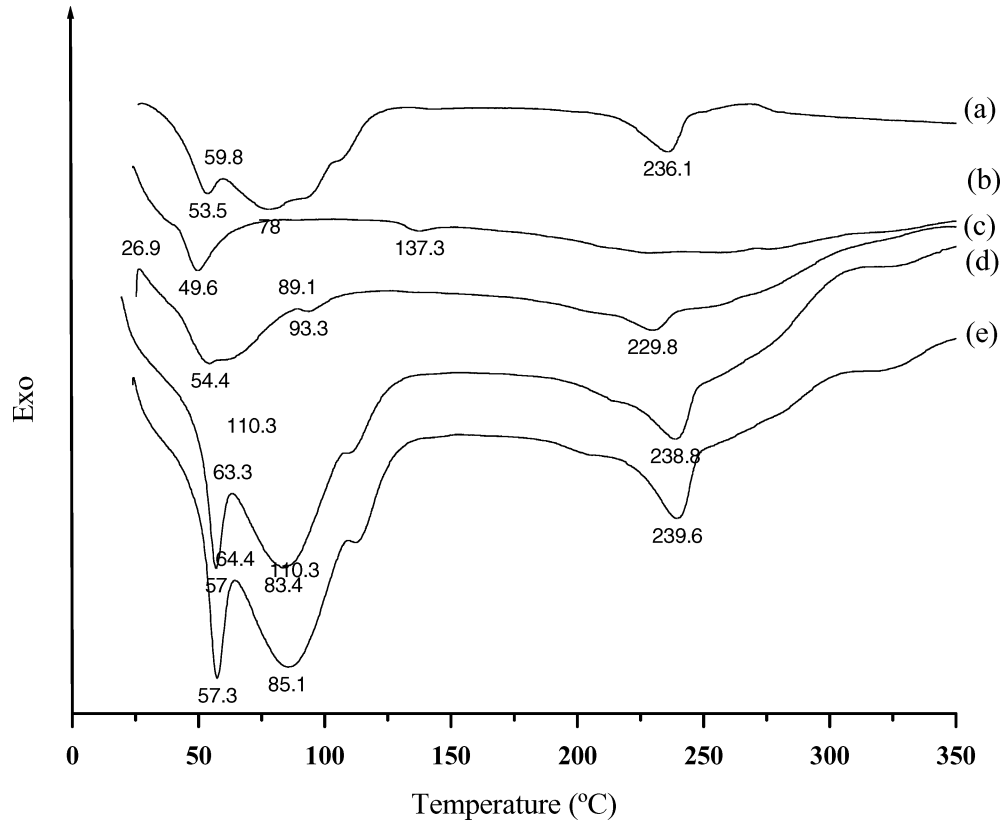

FIG. 4. Thermograms of dehydrated (a) physical mixture 1:1 of chitosan and alginate, (b) physical mixture 1:1 of ALG-CHIT complexes with 0.5% BSA, (c) 1%, (d) 1.5%, and (e) 2% BSA.

334°C but was not observed on ALG-CHIT-BSA complexes. In Figure 4, physical mixtures showed slightly different spectra from polyelectrolyte complexes. The first endothermic peak at 53.5°C of ALG-CHIT complex changed to 57.3°C and its intensity increased with BSA concentration and second endothermic peak at 236°C varied from 229.8 to 239°C depending on the BSA concentration as shown in Figure 4. A similar effect was observed for an additional endothermic peak at 85.1°C. As illustrated in Figure 5, ALG nanospheres showed characteristic endothermic (63°C) and exothermic alginate peaks (259°C). When chitosan was added, spectra demonstrated two separated endothermic peaks, at approximately 76°C and 162°C and an exothermic peak around 266°C. ALG-CHIT-BSA nanospheres showed different spectra where peaks at 162°C and 266°C were not observed and once again an increase of BSA led to more pronounced endothermic peaks.

FT-IR Analysis

Table 2 shows the most pronounced peaks of each sample in the range 1000 to 2000 cm^{-1}. Alginate showed three peaks: 1599 cm^{-1} corresponding to C═O asymmetric stretching, 1410 cm^{-1} to C═O symmetric stretching, and C—O stretching at 1029 cm^{-1}. Chitosan showed two peaks on amide I region at 1696 cm^{-1} and 1637 cm^{-1}; one peak at amide II region at 1543 cm^{-1} corresponding to N-H group, and finally 1409 cm^{-1} to C—N stretching. When chitosan was mixed with alginate, its amide I peaks shifted from 1696 cm^{-1} to 1692 cm^{-1} and from 1637 cm^{-1} to 1633 cm^{-1}; and its amide II band changed from 1543 cm^{-1} to 1549 cm^{-1} with large shoulder corresponding to carbonyl group of alginate. Alginate characteristic peaks at 1410 cm^{-1} and 1029 cm^{-1} shifted after chitosan complexation to 1408 cm^{-1} and 1022 cm^{-1}, respectively. Physical mixture 1:1 of alginate and chitosan showed a different spectrum compared with polyelectrolyte complexes especially C═O group at 1592 cm^{-1}. ALG nanospheres showed a broad band with peaks at 1548, 1409, and 1029 cm^{-1} whereas the CHIT-ALG nanospheres spectrum showed small peak carbonyl group at 1617 cm^{-1}, a strong peak of the amine group at 1540 cm^{-1}, and two more peaks at 1410 and 1019 cm^{-1}.

FT-IR analysis was difficult in the presence of BSA because the noise during analysis was higher. BSA characteristic peaks include 1643–1645 and 1534–1547 cm^{-1} corresponding to amides band I and II, respectively. When BSA was added to ALG-CHIT complexes, new peaks appeared around 1544–1563 and 1455–1458 cm^{-1}. Spectra of physical mixtures were different from isolated polyelectrolytes. BSA-coating led to different spectra showing only a strong dual peak at 1525–1538 and 1559 cm^{-1}.

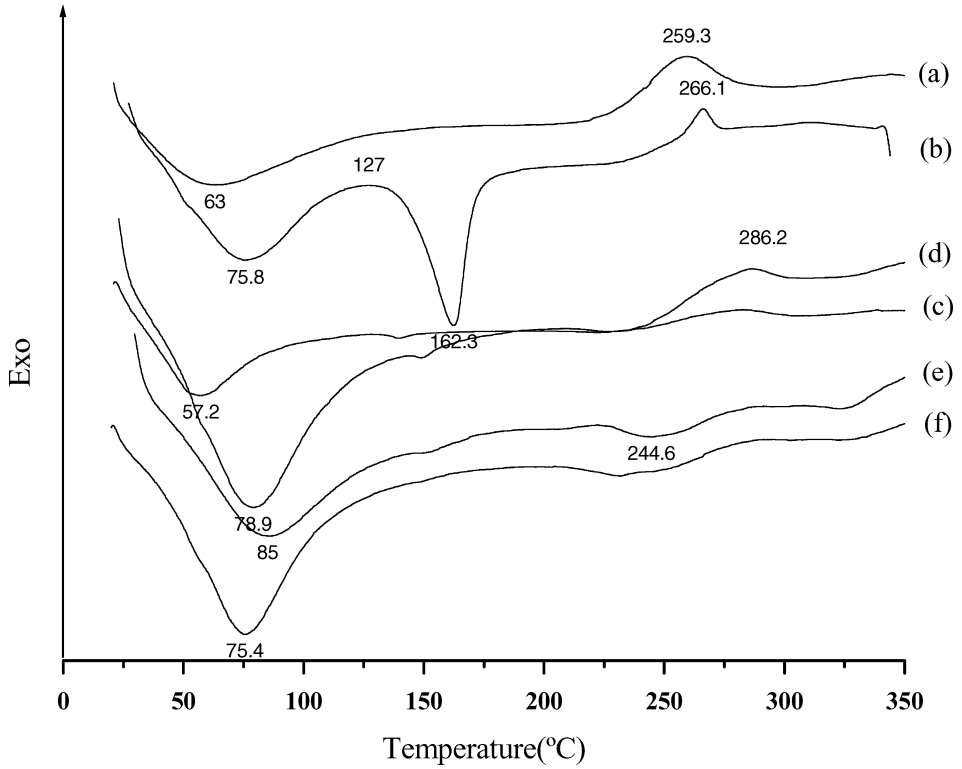

FIG. 5. Thermograms of dehydrated loaded (a) ALG nanospheres, (b) ALG-CHIT nanospheres, (c) ALG-CHIT-BSA nanospheres with 0.5%, (d) 1%, (e) 1.5%, and (f) 2% BSA.

Encapsulation Efficiency

Values of encapsulation efficiency varied from 31 to 90% for the different formulations as seen in Table 3. They were particularly affected by coating parameters ($p < 0.001$). Also, there was no apparent difference between the efficiency values for ALG and CHIT-ALG nanospheres. Encapsulation efficiency decreased with an increase of BSA concentration.

In Vitro Release of Insulin

Figure 6 shows release profiles of insulin from nanospheres under simulated gastrointestinal conditions. At low gastric pH,

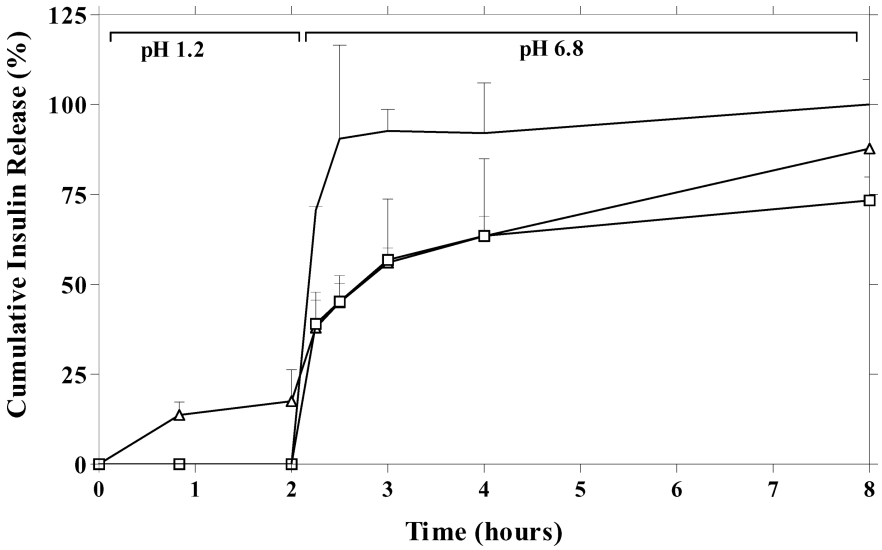

FIG. 6. Release behavior of insulin nanospheres under physiological conditions: ALG (−), ALG-CHIT (–□–), and ALG-CHIT-BSA nanospheres (–Δ–). Each value represents mean ± S.D. ($n = 3$).

TABLE 2
FT-IR analysis of spectra of all tested samples by DSC technique

Compound	C═O Amide I	N─H Amine	C═O asymmetric stretching	N─H Amide II	C═O symmetric stretching or C─N	C─O stretching
Alginate at 2% (w/v)			1599		1410	1029
Chitosan 0.03% (w/v) rich in calcium	1696	1637		1543	1409	
BSA 0.5% (w/v)	1645			1547		
BSA 1% (w/v)	1646			1534		
BSA 1.5 % (w/v)	1646			1547		
BSA 2% (w/v)	1643			1534		
Chitosan–alginate complexes	1692	1633		1549	1408	1022
BSA-chitosan–alginate complexes 0.5% (w/v)	1654		1563	1530	1530	
BSA-chitosan–alginate complexes 1% (w/v)	1655	1633	1544	1534		
BSA-chitosan–alginate complexes 1.5% (w/v)	1655	1642	1554	1541	1455	
BSA-chitosan–alginate complexes 2% (w/v)	1680	1642		1538	1458	
Physical mixture chitosan–alginate	1692	1633	1592	1558	1409	1025
Physical mixture chitosan–alginate+ BSA 0.5% (w/v)	1650	1559				
Physical mixture chitosan–alginate + BSA 1% (w/v)	1650	1559				
Physical mixture chitosan–alginate +BSA 1.5% (w/v)	1654			1543		
Physical mixture chitosan–alginate + BSA 2% (w/v)	1646			1540	1451	
ALG nanospheres			1548		1409	1029
Chitosan-coated nanospheres		1617		1540	1410	1019
ALG-CHIT-BSA nanospheres, BSA 0.5% (w/v)		1559		1538		
ALG-CHIT-BSA nanospheres, BSA 1% (w/v)		1559		1525		
ALG-CHIT-BSA nanospheres, BSA 1.5% (w/v)		1620		1530		
ALG-CHIT-BSA nanospheres, BSA 2% (w/v)		1559		1538		

insulin was fully retained in ALG and ALG-CHIT nanospheres but to a lesser extent with ALG-CHIT-BSA nanospheres. Up to 70%, 40%, and 40% of the insulin was released almost immediately after changing the medium to near neutral pH for ALG, ALG-CHIT, and ALG-CHIT-BSA nanospheres, respectively. ALG-CHIT and ALG-CHIT-BSA nanospheres demonstrated a controlled insulin profile release in simulated intestinal conditions. Full insulin release was only observed with ALG nanospheres after 1 hr.

TABLE 3
Encapsulation efficiency (%) and drug content (%, w/w) of all insulin formulations

Formulation	Parameter	Encapsulation efficiency	Drug content insulin
Dehydrated ALG nanospheres	—	89.9 ± 3.2	2.44 ± 0.01
Dehydrated ALG-CHIT nanospheres	0.03% of chitosan	82.1 ± 5.9	2.23 ± 0.02
Dehydrated ALG-CHIT-BSA nanospheres with 0.03% of chitosan	0.5% of BSA	66.3* ± 5.2	1.82 ± 0.01
	1% of BSA	62.8* ± 1.6	1.71 ± 0.03
	1.5% of BSA	30.9* ± 1.8	0.84 ± 0.02
	2% of BSA	38.5* ± 0.6	1.06 ± 0.05

Each data point represents the mean ± SD from $n = 3$.

*Significant difference from ALG and ALG-CHIT nanospheres: $p < 0.01$.

Insulin Molecular Integrity

To examine the protective ability of the ALG, CHIT-ALG, and ALG-CHIT-BSA nanospheres in the harsh gastric environment, insulin-loaded nanospheres were exposed to pepsin and low pH, and extracted insulin run on HPLC. Nonencapsulated insulin was immediately degraded in the presence of pepsin as seen in Figure 7E. ALG (Figure 7F) and CHIT-ALG nanospheres (Figure 7G) did not protect insulin from peptic digestion as the protein peak was eliminated. Only nanospheres with 0.5% (Figure 7H) and 1% (Figure 7I) BSA coating released intact insulin following pepsin exposure. Insulin peak appeared consistent with intact insulin released from nanospheres and without pepsin incubation as seen in Figure 7D. In contrast, nanospheres with higher levels of BSA coating as seen in Figures 7J and 7K did not release intact insulin and BSA chromatogram zone was gradually degraded with BSA concentration increase.

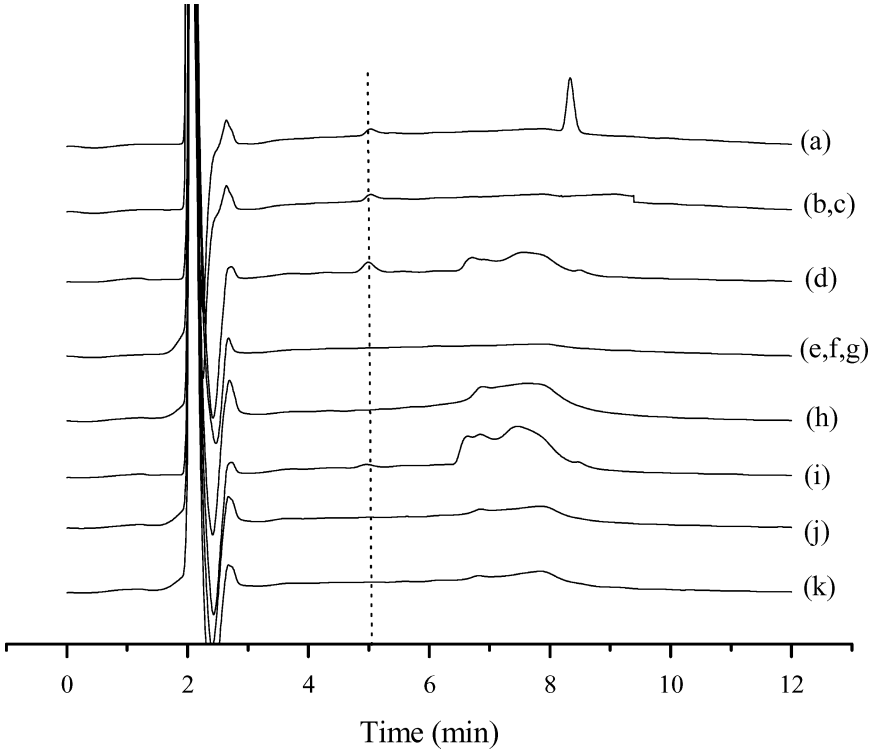

FIG. 7. HPLC curves (a) nonencapsulated insulin, (b, c) insulin encapsulated and released from ALG and ALG-CHIT nanospheres without pepsin incubation, (d) insulin encapsulated and released from ALG-CHIT-BSA nanospheres without pepsin incubation, (e) nonencapsulated insulin after pepsin incubation, (f) insulin encapsulated and released from ALG nanospheres after pepsin incubation, (g) insulin encapsulated and released from ALG-CHIT nanospheres after pepsin incubation, (h) insulin encapsulated and released from ALG-CHIT-BSA nanospheres with 0.5%, (i) 1%, (j) 1.5%, and finally (k) 2% BSA after pepsin incubation. Insulin retention time at 5 min and BSA retention time ~7 min. Additive of commercial insulin is represented by single peak at 8.3 min. This additive is lost after encapsulation and recovery process.

In Vivo Bioassay

Potential use of hydrated and dehydrated nanospheres for oral delivery and its pharmacological effects were evaluated in diabetic rats. Nanospheres formulated of alginate and coated with chitosan and then 1% BSA were used due to their smaller size, higher encapsulation efficiency, and *in vitro* enzymatic protective properties compared with ALG and CHIT-ALG nanospheres. The insulin profile release also was important, but the main objective of this study was to deliver insulin to the intestine, instantaneously or in a controlled pattern, but as a bioactive form.

Oral administration of dehydrated insulin-loaded ALG-CHIT-BSA nanospheres (50 IU/kg) reduced the basal glucose level to 48% as seen in Figure 8. The first reduction of glycemia with dehydrated nanospheres was observed between 2 and 4 hr. Water did not decrease the fasting glycaemia within 8 hr whereas insulin-free ALG-CHIT-BSA nanospheres demonstrated slight glycemia decrease especially to 80 and 74% at 6 and 8 hr, respectively. Fasting plasma glucose levels in all groups did not return to the initial level for any of the conditions tested. The same assay was performed with hydrated insulin-loaded ALG-CHIT-BSA nanospheres. In this case, a stronger hypoglycemic effect to 28% within 12 hr was observed compared with 48% for dehydrated insulin-loaded ALG-CHIT-BSA nanospheres with significant differences from the water group ($p = 0.0579$).

DISCUSSION

Insulin-loaded nanospheres were prepared by nanoemulsion dispersion/*in situ*-triggered gelation. Coating was an important factor in governing the resulting size and shape of the nanospheres. With chitosan-coating, molecular interactions between oppositely charged ALG-CHIT formed larger polymeric particulate networks and ALG alone or ALG-CHIT formed spherical nanospheres. However, subsequent BSA coating results in particle shrinkage. BSA at pH 5.1 was negatively charged interacting with positively charged chitosan (Takahashi et al. 1990) producing a more compact polymer network. A more compact matrix may provide a better exclusion of acid and proteases. Increase of BSA concentration did not lead to an increase in nanosphere diameter. In all cases, particle size was lower than the critical size necessary to enable gastrointestinal absorption by M-cells on Peyer's patches (Norris, Puri, and Sinko 1998; Saez et al. 2000).

DSC and FT-IR showed complex formation between ALG-CHIT-BSA. DSC thermograms of ALG-CHIT-BSA complexes

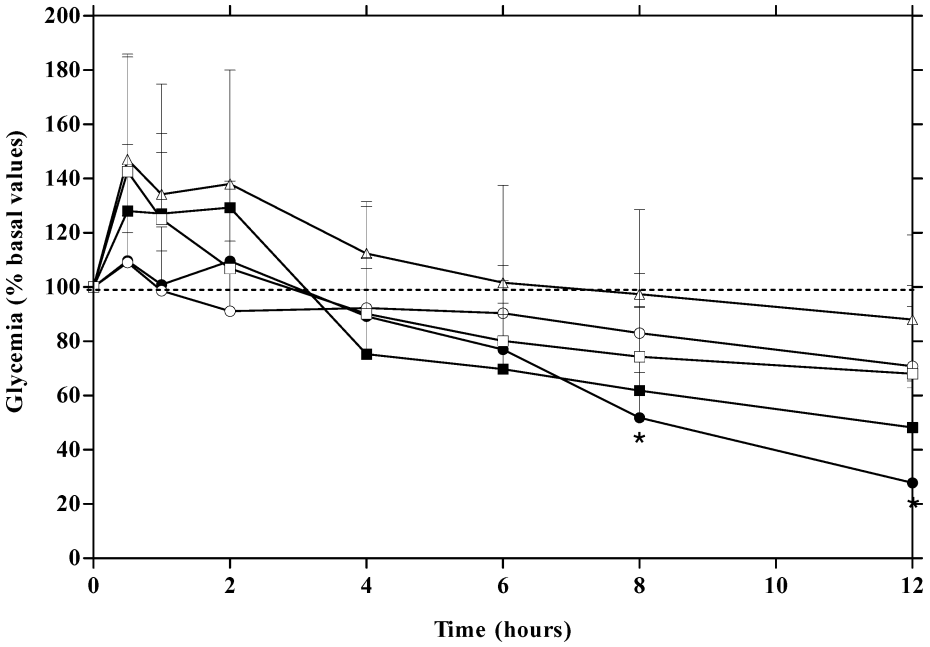

FIG. 8. Blood-glucose levels following oral administration of hydrated insulin-loaded ALG-CHIT-BSA nanospheres (●, $n = 6$), dehydrated insulin-loaded ALG-CHIT-BSA nanospheres (■, $n = 6$), hydrated insulin-free ALG-CHIT-BSA nanospheres (○, $n = 6$), dehydrated insulin-free ALG-CHIT-BSA nanospheres (□, $n = 6$), and water (Δ, $n = 8$) in diabetic male *Wistar* rats fasted for 12 hr. The dose of insulin was 50 IU/kg body weight. Each value represents mean ± S.E.M. *statistically different from water with $p < 0.05$.

were different from isolated polyelectrolyte and ALG-CHIT complexes. DSC thermogram of ALG-CHIT-BSA complexes showed the formation of two endothermic transitions between 50–100°C and 155°C, which may have resulted, respectively, from elimination of water (Smitha, Sridhar, and Khan 2005) and the formation of interactions in polyelectrolyte complex structure. ALG-CHIT-BSA interaction can be characterized by disappearance of the degradation exothermic peak of isolated BSA. Exothermic peaks are usually associated with dehydration, depolymerization, and pyrolitic reactions (Zohuriaan and Shokrolahi 2004).

FT-IR spectra indicates that the peak shifts mainly take place in absorption bands of amine groups of chitosan, amide of BSA, and carboxyl acid groups of alginate, demonstrating electrostatic interaction between ALG-CHIT-BSA. For ALG-CHIT complexes, the asymmetric –C-O- stretching disappeared and a new broad band with strong peak of amine coupled with amide II appeared, indicating that NH_3^+ present in chitosan interacts with $-COO^-$ of alginate. Electrostatic binding resulted between alginate and chitosan, since at working pH, alginate was an anionic polymer in solution (Murata, Miyamoto, and Kawashima 1996) and chitosan was a cationic polymer, and the resulting complex is well documented (Becherán-Marón, Peniche, and Argüelles-Monal 2004; Gaserod, Smidsrod, and Skjak-Braek 1998; Lee, Park, and Ha 1997; Sankalia et al. 2006; Tapia et al. 2004).

There are three types of ionic interactions that contribute to the three-dimensional cross-linked networks of CHIT-ALG nanospheres: the interaction between opposite charges of the biopolymers (electrostatic interactions), the junction formed by the calcium ion, and the guluronic and mannuronic acid units and interchain hydrogen bonds (Sankalia et al. 2006). In ALG-CHIT-BSA complexes, interactions occurred not only between alginate and chitosan, but also between ALG-CHIT and BSA. Complexes between alginate and BSA also have been described in the literature. But in those cases, BSA was used as model protein and not as coating biomaterial (Coppi et al. 2001). These polyelectrolyte complexes are carrying a relatively large number of functional groups that either are charged, or under suitable conditions, can become charged. The formation of polyelectrolyte complexes is mainly driven by an electrostatic mechanism. Charge neutralization and possible local overcompensation or bridging (such as hydrogen bonding, Coulomb forces, van der Waals forces, and transfer forces) are generally mediated by a multivalent counterion that induces attraction between segments of the polyelectrolytes (Sankalia et al. 2006).

Insulin can be incorporated into nanospheres with high efficiency for ALG and CHIT-ALG nanospheres. In both cases, positive amino groups of insulin (pI = 5.3) (Chien 1996) strongly interact with carboxylic groups of alginate (pKa 3.38 and 3.65) (Draget et al. 1994). Data suggest that chitosan coating led to slight decrease of insulin encapsulation efficiency probably due to some destabilization of alginate structure as alginate also interacts with chitosan. The data suggest that BSA coating decreased the encapsulation efficiency of insulin within the nanospheres. Encapsulation efficiency likely involved an additional electrostatic interaction between the positively charged

chitosan and BSA. Thus, it led to an electrostatic competition between BSA and alginate to chitosan and some insulin could be forced out during the coating process.

Insulin release from alginate matrices changed with the choice of coating polymers. First, an absence of insulin release was observed at low pH with ALG nanospheres. Previous work demonstrated that the main reason for protein retention was due to the presence of an addition polyanion in alginate matrix (Silva et al. 2006). The addition of dextran sulphate as another polyanion to alginate matrix increases the polymer concentration which may result in a strong network density. But the effect observed on insulin release at pH 1.2 seemed to be due mainly to electrostatic interactions. Sulfate groups of dextran sulfate will be permanently charged since they have a negative first pK a value and a second pK a value near 2. The presence of negative charges may be responsible for additional interaction with insulin (isoelectric point, pI = 5.3–5.4) at acidic pH, thus preventing its release. This retention was only observed at low pH.

When ALG nanospheres were transferred to intestinal fluid, a complete and fast release of insulin was observed because the alginic acid formed during acid incubation was converted to a soluble salt of sodium alginate causing the matrix to swell and disintegrate. The same low pH profile release was observed with ALG-CHIT nanospheres. In contrast, when ALG-CHIT nanospheres were transferred to intestinal fluid, a controlled insulin release was observed. It seems that chitosan may form a polyelectrolyte complex membrane with alginate possibly serving as a diffusional barrier. These results are in agreement with previous studies where chitosan-coating was able to decrease gel erosion (Murata et al. 1993) allowing sustained release (Polk et al. 1994; Sezer and Akbuga 1999) from alginate microspheres.

In our study, a different profile release occurred with BSA coating. Approximately 15% of insulin was released at low pH and a similar release profile was observed after transfer to pH 6.8. Insulin release at pH 1.2 could be due to an electrostatic competition between all chemical species involved forcing out some insulin during the coating process.

The major objective behind the synthesis of nanospheres was to prepare particles that protected insulin from protease digestion. ALG nanospheres did not offer adequate protection from pepsin probably due to high alginate porosity (Quong and Neufeld 1998). During simulated gastric passage, nanospheres cross a very acidic microenvironment with high proton concentration. Protons diffuse faster than calcium ions present in alginate calcium gel (Quong et al. 1998) forming alginic acid. These protons can alter alginate network structure increasing probability of pepsin-inward diffusion. Chitosan-coated nanospheres should have the advantage of creating an ionic environment that can favor the stabilization of bioactive agents such as insulin (Sajeesh and Sharma 2006). Moreover, chitosan has been described as coating polymer to alter alginate matrix permeability (Quong and Neufeld 1998). Such polyelectrolyte nanospheres displayed suitable protein retention but it provided minimal protease protection, likely because the permeability of alginate matrix was not so well modulated by chitosan.

Intermixing of anionic-cationic–anionic polymers leads to smaller size that can imply a more compact interpolymer network. Smaller size can restrict the intrinsic mobility of individual polymer chains and avoid pepsin diffusion. In addition, most polypeptide drugs, and in particular the nonglycosylated proteins of molecular mass less than 50 kDa such as insulin with 5.8 kDa (Shen and Xu, 2000), are short-lived species *in vivo*, having circulatory half-lives of 5–20 min. In contrast, BSA is described as a stable protein in vivo (Schechter et al. 2005). As in the release profile mechanism, the precise mechanism of insulin enzyme resistance remains unclear. But the observed resistance effect may be due to BSA that serves as degradative target to pepsin, leaving the encapsulated insulin intact.

Finally, blood-glucose levels decreased gradually with orally dosed insulin-loaded nanospheres mainly due to the protective/stabilizing effect of BSA coating. As BSA should be largely degraded in the stomach, the coating on nanospheres being transported into the intestine may begin to break down, initiating the release of entrapped insulin. Oral hypoglycemic effect appeared after 12 hr likely due to the delayed release of insulin following BSA digestion. Also, in this study insulin-free nanospheres had a slight hypoglycemic effect probably because many viscous soluble polysaccharides have been correlated with hypocholesterolemic and hypoglycaemic effects (Burting 2003) and this may be the case of alginate (Ohta et al. 1997). Chitosan also has been used as a hypocholesterolemic and hypoglycaemic agent (Hasegawa et al. 2001) and may be responsible for hypoglycemic effect observed in diabetic rats. Finally, hydrated nanospheres showed a much stronger hypoglycemic effect than did dehydrated nanospheres, likely due to differences in insulin absorption. Some nanosphere agglomeration is expected during lyophylization (Donini et al. 2002) delaying insulin release. Generally, hydrated formulations have an easier dissolution in contact with physiological fluids (Prista, Alves, and Morgado 1995). Consequently, dissolution time is lower than dehydrated formulation.

Hydrated nanospheres showed higher particle size than dehydrated nanospheres, but even so their size was lower than the critical size to be captured by Peyer's patches. As we know, uptake by Peyer's patches is particle size dependent (Reis et al. 2002a). Particles captured by Peyer's patches should have rapid absorption through the lymphatic system and may avoid prehepatic metabolism. At target tissue, for the same time of action, hydrated nanospheres demonstrated a stronger hypoglycemic effect probably due to easier contact with intestinal mucosa. In future work, the hydrated formulation will be subject to further studies to examine nanosphere intestinal absorption.

CONCLUSION

Polyelectrolyte nanospheres show potential as an oral dosage system for insulin and potentially other protein-based drugs.

Insulin nanospheres demonstrated an encapsulation efficiency from 31 to 85% and unimodal size distribution. Generally, 50% of nanospheres have particle size less than 564, 1280, and 144–158 nm for ALG, CHIT-ALG, and ALG-CHIT-BSA nanospheres, respectively. The choice of coating polymer seems to influence insulin release profile and to be crucial to prevent peptic digestion. Only ALG-CHIT-BSA nanospheres with 0.5% and 1% BSA were able to protect and preserve protein stability during pepsin incubation. Optimized formulation consisting of ALG-CHIT-BSA nanospheres with 1% BSA was orally administered to diabetic rats showing a glucose reduction to 48% of initial value within 12 hr. Same formulation but in hydrated state showed higher glucose reduction to 28% of initial value within the same period. ALG-CHIT-BSA nanospheres appear to be a promising delivery vehicle for oral insulin therapy.

REFERENCES

Becherán-Marón, L., Peniche, C., and Argüelles-Monal, W. 2004. Study of the interpolyelectrolyte reaction between chitosan and alginate: Influence of alginate composition and chitosan molecular weight. *Int. J. Biol. Macromol.* 34:127–133.

Boonsongrit, Y., Mitrevej, A., and Mueller, B. W. 2006. Chitosan drug binding by ionic interaction. *Eur. J. Pharm. Biopharm.* 62:267–274.

Burting, P. 2003. Nutrional value of seaweeds. *EJEAFChe* 2:498–503.

Chen, Y., Mohanraj, V. J., and Parkin, J. E. 2003. Chitosan-dextran sulfate nanoparticles for delivery of an anti-angiogenesis peptide. *Let. Pept. Sci.* 10:621–629.

Chien, Y.W. 1996. Human insulin: basic sciences to therapeutic uses. *Drug Dev. Ind. Pharm.* 22:753–789.

Coppi, G., Iannuccelli, V., Leo, E., Bernabei, M. T., and Cameroni, R. 2001. Chitosan-alginate microparticles as a protein carrier. *Drug Dev. Ind. Pharm.* 27:393–400.

Damgé, C., Maincent, P., and Ubrich, N. 2007. Oral delivery of insulin associated to polymeric nanoparticles in diabetic rats. *J. Control. Rel.* 117:163–170.

Damgé, C., Michel, C., Aprahamian, M., and Couvreur, P. 1988. New approach for oral administration of insulin with polyalkylcyanoacrylate nanocapsules as drug carrier. *Diabetes* 37:246–251.

Donini, C., Robinson, D. N., Colombo, P., Giordano, F., and Peppas, N. A. 2002. Preparation of poly(methacrylic acid-g-poly(ethylene glycol)) nanospheres from methacrylic monomers for pharmaceutical applications. *Int. J. Pharm.* 245:83–91.

Draget, K. I., Skjåk-Braek, G., and SmidsrØd, O. 1994. Alginic acid gels: the effect of alginate chemical composition and molecular weight. *Carbohydr. Polym.* 25:31–38.

Gaserod, O., Smidsrod, O., and Skjak-Braek, G. 1998. Microcapsules of alginate-chitosan-I. A quantitative study of the interaction between alginate and chitosan. *Biomaterials* 19:1815–25.

Gursoy, A., and Cevik, S. 2000. Sustained release properties of alginate microspheres and tabletted microspheres of diclofenac sodium. *J. Microencapsul.* 17:565–575.

Hari, P. R., Chandy, T., and Sharma, C.P. 1996. Chitosan/calcium alginate microcapsules for intestinal delivery of nitrofurantoin. *J. Microencapsul.* 13:319–29.

Hasegawa, M., K.Yagi, Iwakawa, S., and Hirai, M. 2001. Chitosan induces apoptosis via caspase-3 activation in bladder tumor cells. *J. Cancer Res.* 92:459–466.

Janes, K. A., Fresneau, M. P., Marazuela, A., Fabra, A., and Alonso, M. J. 2001. Chitosan nanoparticles as delivery system for doxorubicin. *J. Control. Rel.* 73:255–267.

Jerry, N., Anitha, Y., Sharma, C. P., and Sony, P. 2001. In vivo absorption studies of insulin from an oral delivery system. *Drug Deliv.* 8:19–23.

Lee, D. W., Hwang, S.J., Park, J. B., and Park, H. J. 2003. Preparation and release characteristics of polymer-coated and blended alginate microspheres. *J. Microencapsul.* 20:179–92.

Lee, K. Y., Park, W. H., and Ha, W. S. 1997. Polyelectrolyte complexes of sodium alginate with chitosan or its derivatives for microcapsules. *J. Appl. Polym. Sci.* 63:425–432.

Lerco, M. M., Spadella, C. T., Machado, J. L. M., Schellini, S. A., and Pavodini, C. R. 2003. Caracterização de um modelo experimental de*diabetes mellitus*, induzido pela aloxana em ratos. Estudo clínico e laboratorial. *Acta Cirúrg. Brasil* 18:136–142.

Mesiha, M. S., Sidhom, M. B., and Fasipe, B. 2005. Oral and subcutaneous absorption of insulin poly(isobutylcyanoacrylate) nanoparticles. *Int. J. Pharm.* 288:289–293.

Murata, Y., Maeda, T., Miyamoto, E., and Kawashima, S. 1993. Preparation of chitosan-reinforced alginate gel beads—effects of chitosan on gel matrix erosion. *Int. J. Pharm.* 96:139–145.

Murata, Y., Miyamoto, E., and Kawashima, S. 1996. Additive effect of chondroitin sulfate and chitosan on drug release from calcium-induced alginate gel beads. *J. Control. Rel.* 38:101–108.

Norris, D. A., Puri, N., and Sinko, P. J. 1998. Effect of physical barriers and properties on the oral absorption of particulates. *Adv. Drug Deliv. Rev.* 34:135–154.

Ohta, A., Taguchi, A., Takizawa, T., Adachi, T., Kimura, S., and Hashizume., N. 1997. The alginate reduce the postprandial glycaemic response by forming a gel with dietary calcium in the stomach of the rat. *Int. J. Vitam. Nutr. Res.* 67:55–61.

Polk, A., Amsden, B., Yao, K. D., Peng, T., and Goosen, M. F. A. 1994. Controlled release of albumin from chitosan-alginate microcapsules. *J. Pharm. Sci.* 83:178–185.

Prista, L. N., Alves, A. C., and Morgado, R. 1995.. *Tecnologia Farmacêutica*. Lisboa: Fundação Calouste Gulbenkian

Quong, D., and Neufeld, R. J. 1998. DNA protection from extracapsular nuclease, within chitosan-or poly-l-lysine -coated alginate beads. *Biotechnol. Bioeng.* 60:124–134.

Quong, D., Neufeld, R. J., Skjak-Braek, G., and Poncelet, D. 1998. External versus internal source of calcium during the gelation of alginate beads for DNA encapsulation. *Biotechnol. Bioeng.* 57:438–446.

Reis, C. P., Neufeld, R. J., Ribeiro, A. J., and Veiga, F. 2006a. Nanoencapsulation II. Biomedical applications and current status of peptide and protein nanoparticulate delivery systems. *Nanomed. Nanotechnol., Biol. Med.* 2:53–65.

Reis, C. P., Neufeld, R. J., Ribeiro, A. J., and Veiga, F. 2006b. Design of insulin-loaded alginate nanoparticles: influence of calcium ion on polymer gel matrix properties. *Chem. Ind. Chem. Eng. Quart.* 12:47–52.

Reis, C. P., Ribeiro, A. J., Houng, S., Veiga, F., and Neufeld, R. J. 2007. Nanoparticulate delivery system for insulin: design, characterization and in vitro/in vivo bioactivity. *Eur. J. Pharm. Sci.* 30:392–397.

Reis, C. P., Ribeiro, A. J., Neufeld, R. J., and Veiga, F. 2006c. Alginate microparticles as novel carrier for oral insulin delivery. *Biotechnol. Bioeng.* 96:977–989.

Saez, A., Guzman, M., Molpeceres, J., and Aberturas, M. R. 2000. Freeze-drying of polycaprolactone and poly(d,l-lactic-glycolic) nanoparticles induce minor particle size changes affecting the oral pharmacokinetics of loaded drugs. *Eur. J. Pharm. Biopharm.* 50:379–387.

Sajeesh, S., and Sharma, C. P. 2006. Cyclodextrin-insulin complex encapsulated polymethacrylic acid based nanoparticles for oral insulin delivery. *Int. J. Pharm.* 325:147–154.

Sankalia, M., Mashru, R., Sankalia, J., and Sutariya, V. 2006. Reversed chitosan-alginate polyelectrolyte complex for stability improvement of alpha-amylase: optimization and physicochemical characterization. *Eur. J. Pharm. Biopharm.* 65:215–32.

Schechter, Y., Mironchik, M., Rubinraut, S., Saul, A., Tsubery, H., and Fridkin, M. 2005. Albumin-insulin conjugate releasing insulin slowly under

physiological conditions: a new concept for long-acting insulin. *Bioconjug. Chem.* 16:913–920.

Sezer, A. D., and Akbuga, J. 1999. Release characteristics of chitosan treated alginate beads: Ii. Sustained release of a low molecular drug from chitosan treated alginate beads. *J. Microencapsul.* 16:687–696.

Shen, W. H., and Xu, R. J. 2000. Gastrointestinal stability and absorption of insulin in suckling pigs. *Comp. Biochem. Physiol. A Mol. Integr. Physiol.* 125:389–401.

Silva, C. M., Ribeiro, A. J., Ferreira, D., and Veiga, F. 2006. Insulin encapsulation in reinforced alginate microspheres prepared by internal gelation. *Eur. J. Pharm. Sci.* 29:148–159.

Smitha, B., Sridhar, S., and Khan, A. A. 2005. Chitosan-sodium alginate polyion complexes as fuel cell membranes. *Eur. Polym. J.* 41:1859–1866.

Takahashi, T., Takayama, K., Machida, Y., and Nagai, T. 1990. Characteristics of polyion complexes of chitosan with sodium alginate and sodium polyacrylate. *Int. J. Pharm.* 61:35–41.

Tapia, C., Escobar, Z., Costa, E., Sapag-Hagar, J., Valenzuela, F., Busualto, C., Gai, M. N., and Yazdani-Pedram, M. 2004. Comparative studies on polyelectrolyte complexes and mixtures of chitosan-alginate and chitosan-carrageenan as prolonged diltiazem clorhydrate release systems. *Eur. J. Pharm. Biopharm.* 57:65–75.

Tiyaboonchai, W., Woiszwillo, J., Sims, R. C., and Middaugh, C. R. 2003. Insulin containing polyethylenimine-dextran sulfate nanoparticles. *Int. J. Pharm.* 255:139–151.

Zohuriaan, M. J., and Shokrolahi, F. 2004. Thermal studies on natural and modified gums. *Polym. Test.* 23:575–579.